(*35*). In some instances, this approach may fail because of a breakdown of the galvanic assumption, and a direct integral equation modeling approach to remove bathymetric distortion is required (*37*). A tensor decomposition (*35*) was fit to the data but found to have little effect at all periods. In fact, the uncorrected MT tensor displays most of the characteristics of a 2D medium with a strike direction coincident with that of the ridge.

23. J. T. Smith and J. R. Booker, *J. Geophys. Res.* **96**, 3905 (1991).
24. For the inversion algorithm to achieve satisfactory convergence, the target error level has to be larger than 1 SD, probably due to the influence of local topography that is not incorporated in the model, especially large-scale, fault-controlled valleys and seamounts. This is especially true for the apparent resistivity due to static shift, in which the observed amplitude is uncertain by a frequency-independent scale factor. For this reason, error levels on apparent resistivity were increased by a factor of 3 to emphasize fitting the phase. Other inversions were also carried out placing different relative weights on the observed apparent resistivities and phases and selectively downweighting stations that are close to large local topographic features to ensure that the first-order deep structures are retrieved regardless of error levels and achieved misfit value. In addition, the preferred model was derived by setting error thresholds of 5% on apparent resistivity and 5% on phase; this means that individual error estimates smaller than the prescribed threshold are increased to this value, but are left unaltered otherwise.
25. The electromagnetic distortion was computed numerically from the measured bathymetry (*9*) using a thin sheet of spatially variable conductance to simulate depth variations of the ocean. The area between longitudes 110°W and 115°W and latitudes 15°S and 18°S was discretized into 2-km by 2-km square cells and converted into a conductance map. The conductance in a given cell is simply the water depth times an average seawater conductivity of 3.3 S/m. The bathymetric distortion model also depends on the conductivity structure of the mantle, but previous work has shown that mutual coupling between surficial inhomogeneities and deep-mantle lateral heterogeneities is weak (*38*). Hence, the distortion is primarily a function of the sea-floor topography, and a 1D mantle model suffices for the stripping process. This model includes a 50-km-thick lithosphere of resistivity 1000 ohm-m overlying a more conductive mantle with a resistivity decreasing monotonically from 200 ohm-m beneath 50 km and terminating in a 1 ohm-m half-space below 600 km. The confidence intervals on the corrected MT tensor were calculated using the nonparametric jackknife (*33*).
26. J. H. Filloux, *Rev. Geophys.* **17**, 282 (1979); G. Fischer and B. V. LeQuang, *Geophys. J. R. Astron. Soc.* **67**, 257 (1981).
27. The χ^2 misfit measures the difference between the observed and calculated real and imaginary parts of the TE and TM impedances. The penalty function minimized is the sum of the χ^2 misfit plus the squared norm of the log conductivity gradient multiplied by a damping parameter adjusted so that the regularizing term is not overemphasized.
28. S. C. Constable, T. J. Shankland, A. Duba, *J. Geophys. Res.* **97**, 3397 (1991).
29. D. Lizarralde *et al.*, *ibid.* **100**, 17837 (1995).
30. S. J. Mackwell and D. L. Kohlstedt, *ibid.* **95**, 5079 (1990).
31. Q. Bai and D. L. Kohlstedt, *Nature* **357**, 672 (1992).
32. A. D. Chave and D. J. Thomson, *J. Geophys. Res.* **94**, 14215 (1989); _____, in preparation.
33. D. J. Thomson and A. D. Chave, in *Advances in Spectral Analysis and Array Processing*, S. Haykin, Ed. (Prentice-Hall, Englewood Cliffs, NJ, 1991), pp. 58–113.
34. R. W. Groom and R. C. Bailey, *J. Geophys. Res.* **94**, 1913 (1989).
35. A. D. Chave and J. T. Smith, *ibid.* **99**, 4669 (1994).
36. S. N. White, A. D. Chave, J. H. Filloux, *J. Geomagn. Geoelectr.* **49**, 1373 (1997).
37. G. Vasseur and P. Weidelt, *Geophys. J. R. Astron. Soc.* **51**, 669 (1977); R. Nolasco *et al.*, *J. Geophys. Res.* **103**, 30287 (1998).
38. M. Menvielle, J. C. Rossignol, P. Tarits, *Phys. Earth Planet. Int.* **28**, 118 (1982); P. Tarits and M. Menvielle, *Can. J. Earth Sci.* **20**, 537 (1983); A. Terra, thesis, Université de Paris VII (1993).
39. D. R. Bell and G. R. Rossman, *Science* **255**, 1391 (1992).
40. J. J. Roberts and J. A. Tyburczy, *J. Geophys. Res.* **104**, 7055 (1999).
41. We thank K. Baba, L. Banteaux, J. Bailey, A. Dubreule, T. Goto, R. Handy, H. Moeller, R. Petitt, B. Perkins, D. Shinn, and R. Walker for technical assistance. We also thank R. Detrick, G. Hirth, S. Webb, and two anonymous reviewers for helpful comments. U.S. instrumentation and participation in the MELT Experiment was funded by NSF grants OCE-9300117 and OCE-9402324, respectively. French participation was made possible by support from CNRS-INSU and by technical support from DT-INSU, Garchy. Australian support came from Australian Research Council grant A39331792 and a Queen Elizabeth II fellowship. Japanese scientists were supported by grant 07041089 from the ministry of Education, Culture and Science.

25 June 1999; accepted 8 September 1999

Subtropical North Atlantic Temperatures 60,000 to 30,000 Years Ago

Julian P. Sachs* and Scott J. Lehman

A reconstruction of sea surface temperature based on alkenone unsaturation ratios in sediments of the Bermuda Rise provides a detailed record of subtropical climate from 60,000 to 30,000 years ago. Northern Sargasso Sea temperatures changed repeatedly by 2° to 5°C, covarying with high-latitude temperatures that were previously inferred from Greenland ice cores. The largest temperature increases were comparable in magnitude to the full glacial-Holocene warming at the site. Abrupt cold reversals of 3° to 5°C, lasting less than 250 years, occurred during the onset of two such events (Greenland interstadials 8 and 12), suggesting that the largest, most rapid warmings were especially unstable.

Annually dated records of isotope paleotemperature from Greenland ice cores depict a highly volatile climate during the last glacial period [80,000 to 10,000 years ago (ka)] (*1*). Many of the largest temperature excursions occurred from 60 to 30 ka during marine isotope stage (MIS) 3, an interval characterized by intermediate ice sheet size, high-latitude radiation receipts, and atmospheric CO_2 concentrations. Similar excursions are seen in faunal records of high-latitude sea surface temperature (SST) (*2*) and geochemical records of deep ocean ventilation (*3, 4*), consistent with numerical modeling results showing a large dependence of high-latitude sea and air temperatures on the rate and mode of ocean thermohaline circulation (*5*). There are also indications of related SST change at lower latitudes (*6–8*), but these are primarily based on planktonic foraminiferal isotope records that may be influenced by factors other than temperature. The SST of the warm ocean is nonetheless expected to play a crucial role in amplifying and propagating climate change because the partial pressure of water vapor, an abundant and effective greenhouse gas, depends exponentially on temperature (*9*). Here, we present alkenone-derived SST records from Bermuda Rise sediments in the northwest Sargasso Sea and from high-deposition rate sites in the southwest Sargasso Sea in order to evaluate the temperature history of the subtropical Atlantic Ocean during MIS 3.

The Bermuda Rise is a sediment drift deposit northeast of the islands of Bermuda. Lateral sediment focusing within the North American Basin augments deposition at the site (*10*), so that late Quaternary sedimentation rates range from 10 to 200 cm/1000 years (1 ky) (*11*), some 5 to 100 times the open ocean average. As a result, Bermuda Rise sediments provide exceptional resolution in time. Core MD95-2036 (from 33°41.444′N, 57°34.548′W, at a water depth of 4462 m) is 52.7 m in length and contains sediments of Holocene through penultimate glacial (MIS 6) age (*11*). We determined SSTs by alkenone paleothermometry (*12*) in contiguous 1- or 2-cm intervals throughout the 12-m section of the core corresponding to MIS 3. Sedimentation rates averaged 30 cm/ky during the interval, so that single samples represent 33 to 67 years of deposition on average.

Lipids were extracted from 1 to 4 g of freeze-dried sediment with a pressurized fluid extractor, and alkenone abundances were quantified by gas chromatography with flame-ionization detection (*13*). Down-core results are presented in Fig. 1 in units of the alkenone unsaturation ratio ($U^{k'}_{37}$) and as estimated SSTs from the regression relation of Prahl and others (*12, 14*). Our semiautomated analytical procedure allows the routine analysis

Institute of Arctic and Alpine Research, University of Colorado, Boulder, CO 80309–0450, USA.

*Present address: Department of Environmental Science, Barnard College, Columbia University, 3009 Broadway, New York, NY 10027, USA.

of 50 samples per week with an external precision of 0.0058 $U^{k'}_{37}$ units (0.17°C) (*15*). Dispersion of duplicate measurements in the interval from 2750 to 3000 cm exceeds the external precision because of a contamination problem that was encountered and eliminated early in our study (*16*).

Reconstructed SSTs ranged from ~15.5° to 21°C during MIS 3 and are associated with changes in sediment lightness (Fig. 1), a proxy for the $CaCO_3$ content of the sediment at this location that has been previously correlated to the Greenland record of paleotemperature (*11*). Millennium- to century-scale SST minima (stadials) were typically between 15.5° and 17°C, and maxima (interstadials) were between 19° and 21°C. The mean warming from stadial minima to interstadial maxima for 12 millennium-scale SST oscillations was 3.1°C (a range of 1.7° to 5.3°C). In addition, stadial minimum temperatures reached successively colder levels during MIS 3, from 17.3°C before interstadial 15 (IS-15) to 15.3°C before IS-5. The large SST changes documented in core MD95-2036 are consistent with ~1–per mil millennial variations in planktonic foraminiferal $\delta^{18}O$ measured in nearby core KNR31-GPC5 from the Bermuda Rise (*8*), although there are notable differences in the two proxy records that suggest either an important salinity influence on the planktonic $\delta^{18}O$ (*17*) or changes in the season or depth of foraminiferal calcification.

Our temperature estimates are largely insensitive to the regression relation used to convert $U^{k'}_{37}$ values to SST. For example, a calibration from a recent global compilation of core-top and contemporary mean annual SSTs (*18*) yields results that are nearly identical to those we obtained using a relation (*12*) based on culture experiments (*14*). In addition, measurements of box-core samples spanning the past 2500 years of sedimentation at the Bermuda Rise yield an average SST of 21.8° ± 0.5°C (n = 49) with the culture relation (*19*). Considering that this interval includes the Little Ice Age cold excursion (*20*), the 2500-year average is close to the modern annual mean and production-weighted SSTs at 0 m of 22.8° and 22.5°C, respectively (*21*). Changes in the contribution of fine-grained sediment to the site have not influenced measured $U^{k'}_{37}$ values (*22*).

Reconstructed millennium- and century-scale SST oscillations at the Bermuda Rise are unexpectedly large in light of climate proxy data (*23*) and numerical models (*24*) indicating 2° to 5°C of warming between full glacial and present-day or Holocene–average temperatures in the region. In order to determine whether such variations were a local response to the movement of an oceanographic front or were associated with more widespread temperature change, we also measured $U^{k'}_{37}$ ratios across selected events in cores from the Blake (KNR140-JPC27; from 30°01′N, 73°36′W, water depth of 3975 m) and Bahama (KNR31-GPC9; from 28°15′N, 74°26′W, water depth of 4758 m) outer ridges, in the southwestern Sargasso Sea (Fig. 2). SSTs rose abruptly by 2° to 2.5°C during the transitions into IS-8, IS-12, and IS-14 at both locations (*25*), equivalent to one-half the warming observed at the Bermuda Rise (Fig. 1). Absolute SSTs in the southwestern Sargasso Sea were higher than those at the

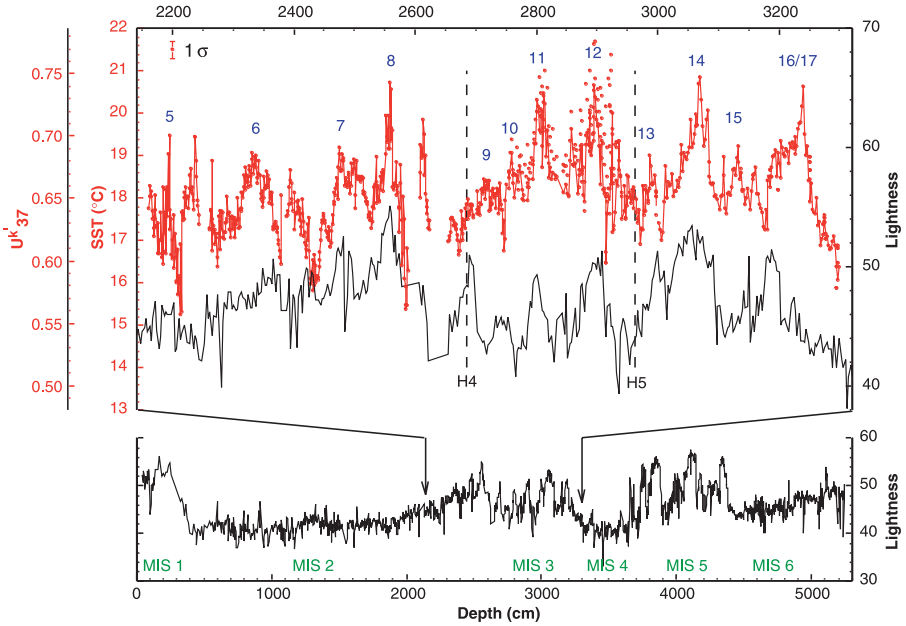

Fig. 1. Alkenone-derived SSTs (red circles) and sediment lightness values (a proxy for the $CaCO_3$ content of the sediment) (black lines) shown to depth in Bermuda Rise core MD95-2036, with an expanded view of results for MIS 3 (60 to 30 ka). $U^{k'}_{37}$ values were converted to SST with the equation $U^{k'}_{37} = 0.034T + 0.039$ (*12, 14*). The precision of the analysis (1σ error bar) is 0.00585 $U^{k'}_{37}$ units or 0.17°C. Scatter between 2750 and 3000 cm is the result of contamination by partially coeluting compounds (*16*). Warm interstadial events (numbered in blue) were identified on the basis of visual correlation to the GISP2 isotope temperature record (*1*). Two ice-rafted debris (IRD) maxima in Bermuda Rise sediment cores, corresponding to Heinrich events 4 and 5 (H4 and H5) (*8*), are also shown (vertical dashed lines).

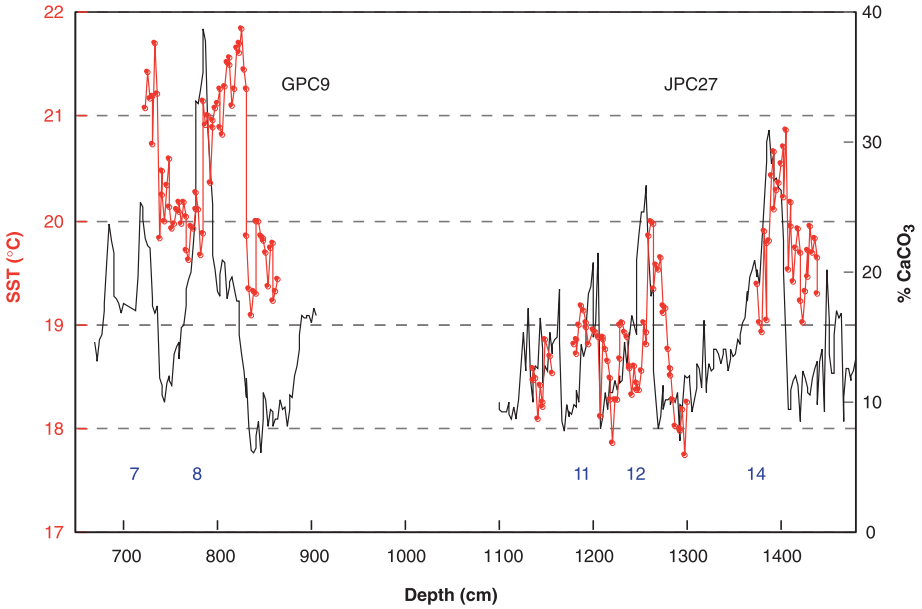

Fig. 2. Alkenone-derived SSTs (red circles) and $CaCO_3$ content of the sediment (black line) for two sites in the southwestern Sargasso Sea. The $CaCO_3$ content of the sediment was used to identify the position of interstadial events (blue numbers) (*25*). SSTs rose abruptly at the onset of IS-7 and IS-8 at the Blake Outer Ridge (core KNR31-GPC9; 28°15′N, 74°26′W) and at the onset of IS-11, IS-12, and IS-14 at the Bahama Outer Ridge (core KNR140-JPC27; 30°01′N, 73°36′W). The amplitude of warming was about half that at the Bermuda Rise in the northern Sargasso Sea.

Bermuda Rise throughout the studied intervals. At the Blake Outer Ridge, stadial cool episodes were warmer by 1° to 1.5°C, and at the Bahama Outer Ridge, the stadials were warmer by 2° to 3.5°C. In contrast, maximum interstadial temperatures at both southwestern locations were within 0.5° to 1.0°C of those at the Bermuda Rise for coeval events. The larger divergence of lower latitude SSTs from those at the Bermuda Rise during cold periods suggests that diminished poleward heat transport contributed to stadial cooling, an expected consequence of weakened thermohaline circulation (*26*). SST relations among these study sites thus support the interpretation of Bermuda Rise SSTs in terms of a regional climatic signal rather than a localized response to the movement of an oceanographic front.

To place SST results from core MD95-2036 on an estimated age scale, we correlated variations in sediment lightness with weight-percent $CaCO_3$ variations in core KNR31-GPC5 (correlation coefficient $r = 0.90$), previously dated with radiocarbon and oxygen isotopic stage boundaries (*3*). However, this method produced ages for the SST events that were 2000 to 5000 years older than their apparent counterparts in Greenland paleotemperature ($\delta^{18}O$ of ice, $\delta^{18}O_{ice}$) records, probably due to radiocarbon dating errors associated with carbonate dissolution and poor calibration and to uncertainties in the SPECMAP age scale (*27*). We therefore developed an alternative age model by maximizing the correlation between Bermuda Rise SSTs and layer-counted variations in Greenland $\delta^{18}O_{ice}$. Using 146 tie points, we obtained a correlation coefficient of 0.83 between the two series (*28*). This correlation results in a linear relation of amplitude between the two paleotemperature records (Fig. 3A); all major variations in the ice core are observed at the Bermuda Rise.

Although this age model lacks absolute chronologic control, on the basis of the linear covariation of millennium- and century-scale features, we reason that it provides the best possible estimate of relative age. We know of no mechanism by which to delay the climate signal while preserving the linear relation of amplitude for both brief and long-lasting events (Fig. 3A). Furthermore, because the heat capacity and mixing time of the atmosphere are small with respect to those of the ocean, the atmospheric adjustment to such large oceanic changes is expected to be nearly instantaneous, on the order of days to years. Absolute uncertainty of the time scale is approximated by the error associated with counting annual layers in the Greenland Ice Sheet Project 2 (GISP2) ice core, which is 5% (*29*), or 1500 to 3000 years in MIS 3. Relative uncertainty of the SST chronology is 10 to 100 years during stadial cool episodes, when inferred resolution and sedimentation rates (Fig. 3D) are high, and 100 to 1000 years during interstadial warm periods, when inferred resolution and sedimentation rates are low (*30*).

The inferred amplitude lock of the SST and $\delta^{18}O_{ice}$ series (Fig. 3A) suggests that Bermuda Rise SST variations were one-third to one-half of Greenland air temperature variations, depending on the $\delta^{18}O_{ice}$-temperature relation used to estimate isotopic paleotemperature (*31*). The SST record also contains abrupt features not yet identified in the ice core. The most important of these are large (3° to 5°C) oscillations that interrupt rapid warmings at the onset of IS-8 and IS-12 (Fig. 3, B and C). These events probably occurred entirely within the stadial-interstadial transitions marked by $\delta^{18}O_{ice}$ in GISP2 and Greenland Ice Core Project (GRIP) ice cores, a period of not more than 250 years (*28*). Estimated rates of sedimentation, as determined by correlation to GISP2, rose during these transitions (Fig. 3D), whereas associated SSTs sank to minima that were substantially colder than preceding stadial temperatures (Fig. 3B). We thus speculate that transitional cooling episodes were associated with enhanced meltwater and iceberg delivery of sediment to the North Atlantic Basin during Heinrich events 5 and 4 (at the onsets of IS-12 and IS-8, respectively) (*2*) and consequent meltwater suppression of North Atlantic thermohaline circulation (*4, 32*). A limited number of benthic foraminiferal Cd/Ca measurements from IS-8 in core MD95-2036 and additional Cd/Ca and $\delta^{13}C$ measurements from correlative levels in core KNR31-GPC5 support diminished rates of North Atlantic Deep Water formation during Heinrich event 4 (*8*). Similarly abrupt climatic shifts and deep ocean changes have been previously inferred in association with this event in both the subpolar North Atlantic (*2, 32*) and the western equatorial Atlantic (*7*).

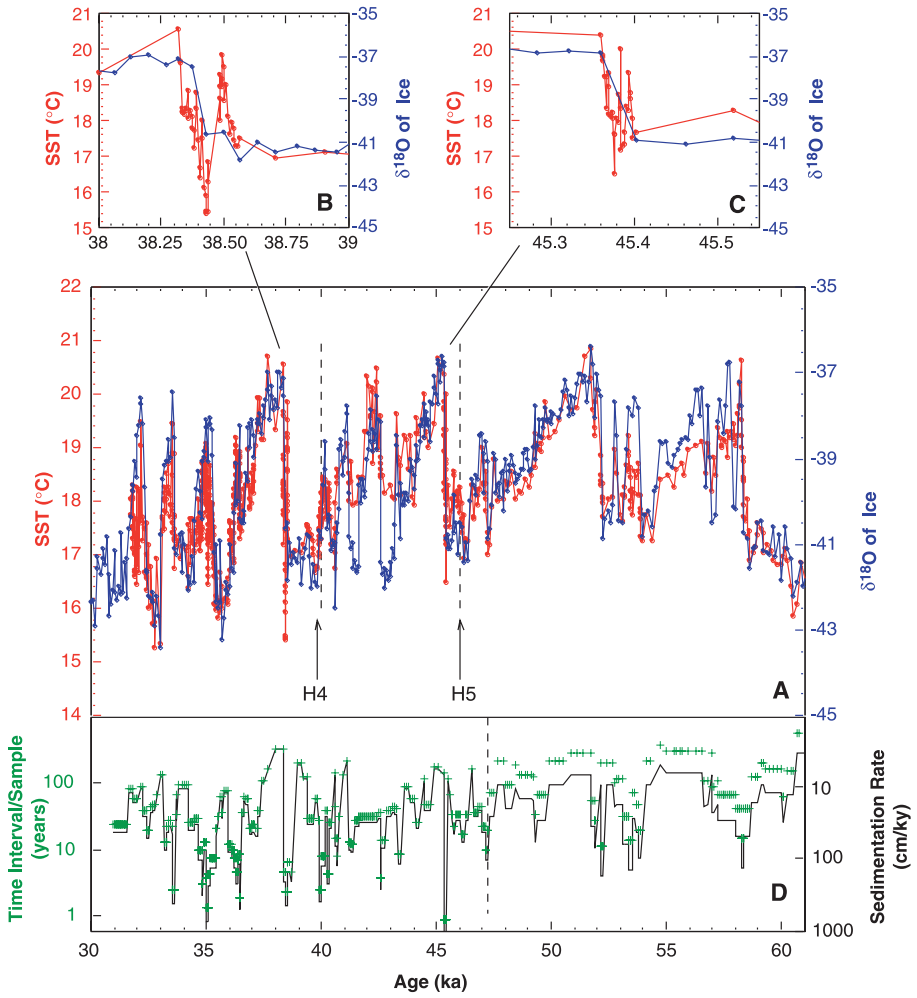

Fig. 3. (**A**) Bermuda Rise SSTs (red circles) and central Greenland $\delta^{18}O_{ice}$ (blue diamonds) for MIS 3 on the GISP2 ice core time scale (*28*). The position of IRD peaks associated with Heinrich events 4 and 5 in the sediment core is shown for stratigraphic reference (dashed vertical lines). Cold reversals of 3° to 5°C occur during the onset of (**B**) IS-8 and (**C**) IS-12 in less than 250 years. (**D**) High instantaneous rates of sedimentation (black line) of 100 to 1000 cm/ky characterize cold stadial periods and the transitions into interstadials, and interstadial periods are characterized by lower sedimentation rates of 3 to 10 cm/ky. The sampling interval was 2 cm before 47.2 ky B.P. (dashed vertical line) and 1 cm afterward. The interval of time represented by each sample (green crosses) varies from ~1 to 20 years during stadial periods to 100 to 300 years during interstadials.

Our results demonstrate that large millennium- to century-scale changes in SST were not restricted to the polar and subpolar North Atlantic, but extended well into the subtropics. Indeed, rapid SST changes in the northern and southwestern Sargasso Sea (2° to 5°C and 1° to 2.5°C, respectively) were as large or larger than full glacial-Holocene mean annual SST differences reconstructed by the CLIMAP (Climate: Long-Range Investigation, Mapping, and Prediction) project (*23*) with foraminiferal transfer functions. They are also comparable to alkenone-derived SSTs from Bermuda Rise core KNR31-GPC5, indicating a deglacial temperature increase of 5.4°C (from 16.5° to 21.9°C) (*33*). Amplitudes of the largest MIS 3 SST events in the subtropical North Atlantic have a distribution similar to that observed in a number of coupled atmosphere-ocean models simulating SSTs for Last Glacial Maximum versus modern boundary conditions (*24*). The presence of such large SST variations over the warm ocean may help to explain observations of abrupt climate events at locations distant from the subpolar North Atlantic and Greenland [for example, (*6, 34*)] through direct thermal forcing and the temperature–water vapor feedback.

References and Notes

1. P. M. Grootes, M. Stuiver, J. W. C. White, S. Johnsen, J. Jouzel, *Nature* **366**, 552 (1993); P. M. Grootes and M. Stuiver, *J. Geophys. Res.* **102**, 26455 (1997).
2. G. Bond *et al.*, *Nature* **360**, 245 (1992); G. Bond *et al.*, *ibid.* **365**, 143 (1993).
3. L. D. Keigwin and G. A. Jones, *J. Geophys. Res.* **99**, 12397 (1994).
4. D. W. Oppo and S. J. Lehman, *Paleoceanography* **10**, 901 (1995); C. D. Charles, J. Lynch-Stieglitz, U. S. Ninnemann, R. G. Fairbanks, *Earth Planet. Sci. Lett.* **142**, 19 (1996); L. Vidal *et al.*, *ibid.* **146**, 13 (1997); R. Zahn *et al.*, *Paleoceanography* **12**, 696 (1997); J. F. McManus, D. W. Oppo, J. L. Cullen, *Science* **283**, 971 (1999).
5. S. Manabe and R. J. Stouffer, *J. Clim.* **1**, 841 (1988); A. Schiller, U. Mikolajewicz, R. Voss, *Report No. 188* (Max-Planck-Institut für Meteorologie, Hamburg, Germany, 1996).
6. I. L. Hendy and J. P. Kennett, *Geology* **27**, 291 (1999).
7. W. B. Curry and D. W. Oppo, *Paleoceanography* **12**, 1 (1997).
8. L. D. Keigwin and E. A. Boyle, *ibid.* **14**, 164 (1999).
9. W. Broecker, *GSA Today* **7**, 1 (1997); R. S. Webb, D. H. Rind, S. J. Lehman, R. J. Healy, D. Sigman, *Nature* **385**, 695 (1997).
10. D. O. Suman and M. P. Bacon, *Deep Sea Res.* **36**, 869 (1989).
11. E. A. Boyle, *Proc. Natl. Acad. Sci. U.S.A.* **94**, 8300 (1997).
12. F. G. Prahl and S. G. Wakeham, *Nature* **330**, 367 (1987); F. G. Prahl, L. A. Muehlhausen, D. L. Zahnle, *Geochim. Cosmochim. Acta* **52**, 2303 (1988).
13. The split sediment core was sampled with standard trace-organic clean procedures. Samples were stored frozen at −20°C and freeze-dried just before extraction. After drying, 1 to 4 g of sediment was weighed, and an equivalent quantity of sodium sulfate (a dispersing agent) and 2 μg of ethyl triacontanoate (a recovery standard dissolved in 20% acetone in hexane) were added. The mixture was loaded into a stainless steel cell and extracted on a Dionex ASE-200 pressurized fluid extractor with methylene chloride at 150°C and 2000 psi for ~25 min. The solvent was evaporated on a Zymark Turbovap II, and the lipid extract was transferred to a 2-ml autosampler vial. The extract was redissolved in 400 μl of toluene containing 2 μg of *n*-hexatriacontane (*n*-C_{36}, a quantitation standard) and derivatized with bis(trimethylsilyl)trifluoroacetamide (Aldrich) at 60°C for 1 hour. C_{37} methyl ketones (alkenones) were quantified by capillary gas chromatography on a Hewlett Packard 6890 with a Chrompack CP-Sil-5 column (60 m by 0.32 mm inner diameter), a programmable temperature vaporization inlet in solvent-vent mode, and flame-ionization detector, all controlled by Hewlett Packard Chemstation software.
14. $U^{k'}_{37}$ = 37:2/(37:2 + 37:3), where 37:2 is the diunsaturated C_{37} methyl ketone, heptatriaconta-15*E*,22*E*-dien-2-one, and 37:3 is the tri-unsaturated C_{37} methyl ketone, heptatriaconta-8*E*,15*E*,22*E*-trien-2-one (*12*). Laboratory cultures of the prymnesiophyte *Emiliania huxleyi* grown at 8° to 25°C produced a linear relation between water temperature (*T*) and $U^{k'}_{37}$ of the form $U^{k'}_{37} = 0.034T + 0.039$, $r^2 = 0.994$ (*12*). A nearly identical relation, $U^{k'}_{37} = 0.033T + 0.044$, $r^2 = 0.958$, was obtained for a worldwide assortment of core-top sediment values ($n = 370$) regressed against associated mean annual 0-m SSTs (range of 0° to 29°C) (*18*), supporting the culture regression (*12*) used in this study.
15. A Bermuda Rise sediment standard (BRA), prepared from a mixture of late Pleistocene glacial and interglacial material, was extracted after every 30 authentic samples. Its $U^{k'}_{37}$ value was determined twice, with 15 samples run between analyses. The mean $U^{k'}_{37}$ of 115 BRA analyses during this study was 0.7300 ± 0.005846 (1σ), or 20.23° ± 0.1720°C. This compares with a mean SST of 20.24° ± 0.1646°C for 47 individual BRA extracts. Thus, analytical precision is dictated by the chromatography.
16. The original sampling protocol included the use of Whirl-Pak plastic sample bags (Nasco, Fort Atkinson, WI) that contaminated the dry sediment with a compound having similar retention characteristics to the 37:3 alkenone. The partial coelution of the two compounds hindered quantification of the alkenone. In instances where the contaminant peak area equaled or exceeded that of the alkenone, the sample was not used for the SST reconstruction. The remaining contaminated samples were analyzed with three different chromatographic methods. The results of all analyses are plotted in Fig. 1, but only those SSTs determined with the optimized final method (that is, those giving the best separation between the contaminant and alkenone) are connected by a line. Only the results of the optimized method are plotted in Fig. 3. In all, 2.5 m, or 250 samples, of the 12-m section studied were affected. When the source of the contaminant was identified, a revised protocol employing precombusted glass sample vials was implemented.
17. The near-constant planktonic $\delta^{18}O$ values characterizing stadial periods and the similar amplitudes of interstadial isotopic depletions differ from the trend of decreasing stadial SSTs and widely varying (2° to 5°C) interstadial warming periods evident in the alkenone record (Fig. 3A). The lack of a trend in isotopic depletion through MIS 3 suggests decreasing salinity during subsequent stadials.
18. P. J. Müller, G. Kirst, G. Ruhland, I. V. Storch, A. Rosell-Mele, *Geochim. Cosmochim. Acta* **62**, 1757 (1998).
19. J. P. Sachs and S. J. Lehman, paper presented at the 6th International Conference on Paleoceanography, Lisbon, 24 to 28 August 1998.
20. L. D. Keigwin, *Science* **274**, 1504 (1996).
21. S. Levitus and T. Boyer, Eds., *Temperature*, vol. 4 of *World Ocean Atlas 1994* (National Oceanographic Data Center, Silver Spring, MD, 1994). Production-weighted SSTs were calculated with flux data from W. G. Deuser, *Deep Sea Res.* **33**, 225 (1986).
22. $U^{k'}_{37}$ values (and estimated SSTs) show a variable phase relation with sediment lightness [(that is, $CaCO_3$ concentrations) (Fig. 1)]. Dilution with continental and Scotian Margin sediment results in low $CaCO_3$ concentrations during periods of harsh climate when sediment advection is most intense (*10*). If changes in $U^{k'}_{37}$ resulted from variable dilution with advected sediment, we would expect estimated SSTs to vary in phase with lightness.
23. CLIMAP Project Members, *Sea-Surface Temperature Anomaly Maps for August and February in the Modern and Last Glacial Maximum*, *Map Chart Sec. MC-36* (Geological Society of America, Boulder, CO, 1981).
24. A. Ganopolski, S. Rahmstorf, V. Petoukhov, M. Claussen, *Nature* **391**, 351 (1998); A. J. Weaver, M. Eby, A. F. Fanning, E. C. Wiebe, *ibid.* **394**, 847 (1998).
25. Carbonate data and identification of interstadial events in cores KNR31-GPC9 and KNR140-JPC27 are from (*3*) and L. Keigwin, unpublished data, respectively.
26. Benthic paleochemical evidence for weakened thermohaline circulation in association with cold stadial episodes during MIS 3 is documented in (*8*) and is expected from numerical climate models (*5*).
27. A similar age discrepancy was previously noted in a comparison of independently dated $CaCO_3$ records from northwestern Atlantic cores KNR31-GPC5 and KNR31-GPC9 (*3*), suggesting that accelerator mass spectrometry ^{14}C dates in the deeper parts of core KNR31-GPC5 may be in error. The estimated error of the SPECMAP age scale is 3.5 to 7.7 ky in MIS 3 [D. G. Martinson *et al.*, *Quat. Res.* **27**, 1 (1987)].
28. The values of $\delta^{18}O_{ice}$ are from (*1*). The ice core time scale was developed by counting annual layers [D. A. Meese *et al.*, *Special CRREL Report 94-1* (Cold Regions Research and Engineering Laboratory, Hanover, NH 1994)] and from a comparison of $\delta^{18}O$ of trapped air to the SPECMAP marine $\delta^{18}O$ time scale [M. Bender *et al.*, *Nature* **372**, 663 (1994)]. Correlation between $\delta^{18}O_{ice}$ (GISP2) and the alkenone SST record in the sediment (core MD95-2036) was accomplished with the LinAge function of the AnalySeries 1.1 toolkit [D. Paillard, L. Labeyrie, P. Yiou, *Eos Trans. Am. Geophys. Union* **77**, 379 (1997)]. This function performs a linear interpolation between tie points.
29. R. B. Alley *et al.*, *J. Geophys. Res.* **102**, 26367 (1997).
30. These are estimates of the uncertainty in graphical correlation between the two time series. High (low) rates of sedimentation during periods of harsh (mild) climate at Bermuda Rise have been documented on the basis of detailed ^{230}Th and ^{14}C measurements [J. F. Adkins and E. A. Boyle, *Eos Trans Am. Geophys. Union* **76** (Fall Meeting Suppl.), F282 (1995); J. Adkins, E. A. Boyle, L. Keigwin, E. Cortijo, *Nature* **390**, 154 (1997); (*20*)], consistent with sediment-climate relations we inferred for MIS 3.
31. The exception to the amplitude lock occurs primarily before and after IS-11 [~41.5 to 43 ky before the present (B.P.)] and, to a lesser extent, during IS-15, IS-16, and IS-17 (~52.5 to 58 ky B.P.). Although we cannot discount a change in the temperature relation between Greenland and the subtropical Atlantic at these times, we note that the former interval was affected by the plastic contamination discussed in (*16*). Several $\delta^{18}O_{ice}$-temperature relations have been derived for central Greenland, variously based on spatial [W. Dansgaard, *Tellus* **16**, 436 (1974); J. Jouzel, R. D. Koster, R. J. Suozzo, G. L. Russell, *J. Geophys. Res.* **99**, 25791 (1994)], temporal [C. A. Shuman *et al.*, *J. Geophys. Res.* **100**, 9165 (1995)], and borehole [K. M. Cuffey *et al.*, *Science* **270**, 455 (1995)] calibrations and on the thermal diffusion of N isotopes [J. P. Severinghaus, T. Sowers, E. J. Brook, R. B. Alley, M. L. Bender, *Nature* **391**, 141 (1998)]. The slope (α) of these relations varies by up to a factor of 2. The larger response of Greenland air temperature in relation to Bermuda Rise SST results from the greater sensitivity of high-latitude sea and air temperatures to changing thermohaline circulation [compare (*5*)].
32. M. R. Chapman and N. J. Shackleton, *Earth Planet. Sci. Lett.* **159**, 57 (1998).
33. S. J. Lehman, N. Weicker, T. Eglinton, *Eos Trans. Am. Geophys. Union* **73** (Fall Meeting Suppl.), 259 (1992).
34. E. C. Grimm, G. L. Jacobson Jr., W. A. Watts, B. C. S. Hansen, K. A. Maasch, *Science* **261**, 198 (1993); T. V. Lowell *et al.*, *ibid.* **269**, 1541 (1995).

35. We thank L. Keigwin for sediment samples and $CaCO_3$ data from the Blake and Bahama Outer Ridges and for thoughtful discussions, E. Boyle, the Institut Français pour la Recherche et la Technologie Polaires and International Marine Global Change Study coring program, the captain and crew of the research vessel *Marion Dufresne* for acquiring and facilitating our access to core MD95-2036, and T. Kernan for assistance. This work was funded by NSF grant ATM 9610128 to S.J.L.

9 August 1999; accepted 16 September 1999